

OrcVIO: Object residual constrained Visual-Inertial Odometry

Mo Shan Qiaojun Feng Nikolay Atanasov

Existential Robotics Laboratory
Department of Electrical and Computer Engineering
University of California, San Diego

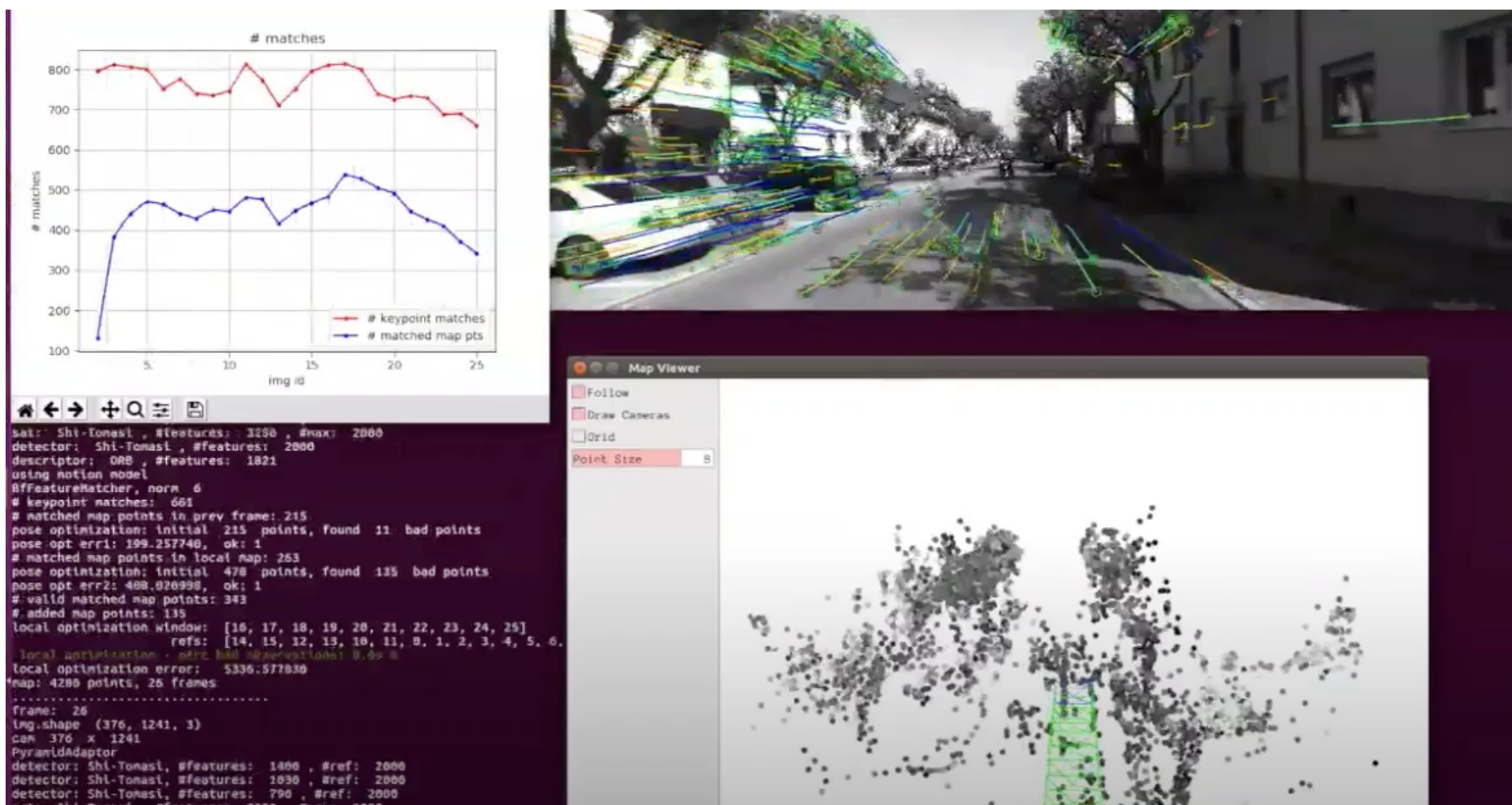


UC San Diego
JACOBS SCHOOL OF ENGINEERING
Electrical and Computer Engineering

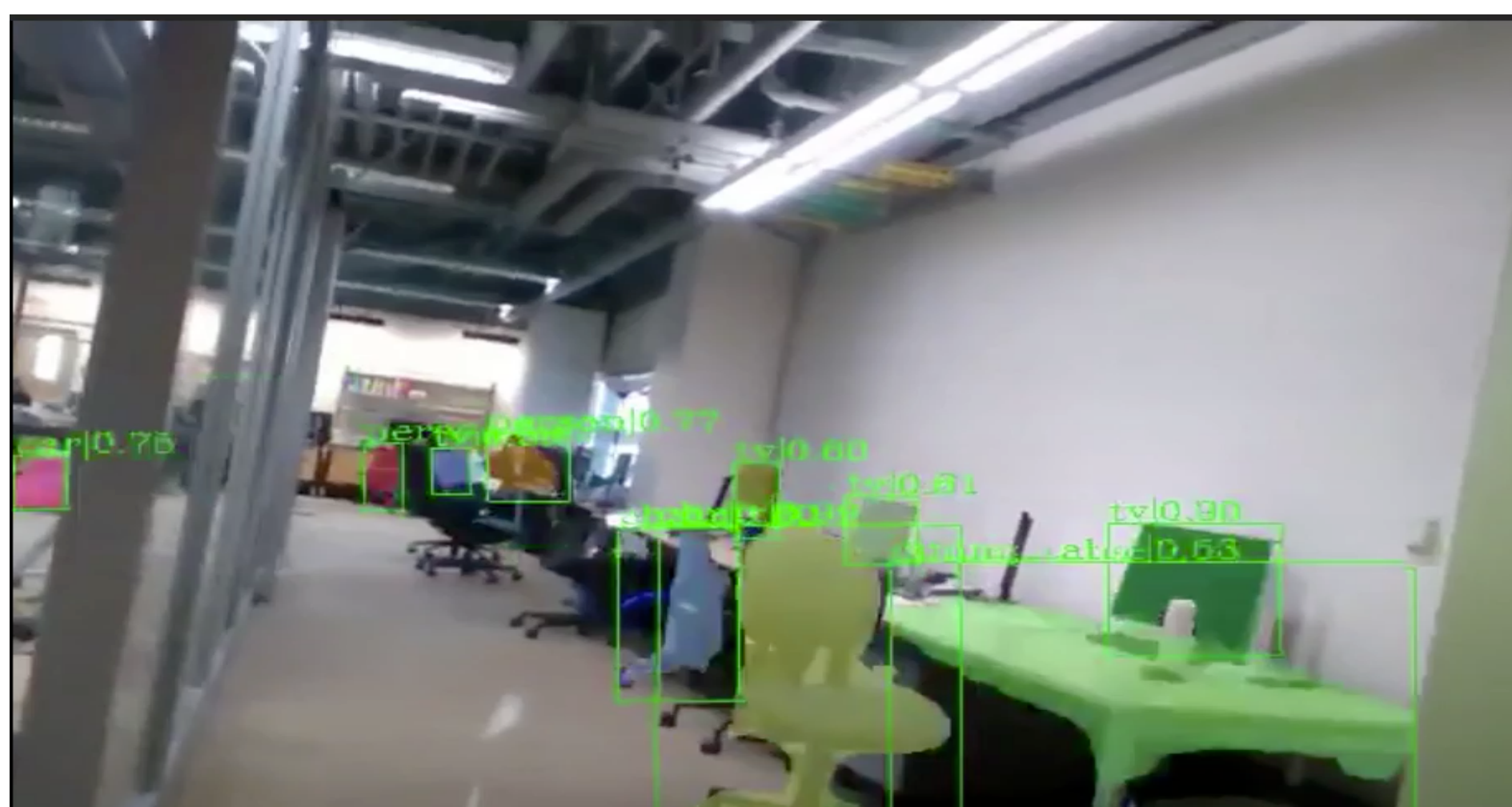
CONTEXTUAL
ROBOTICS
INSTITUTE

Motivation

- Most SLAM/VIO methods produce geometric environment representations



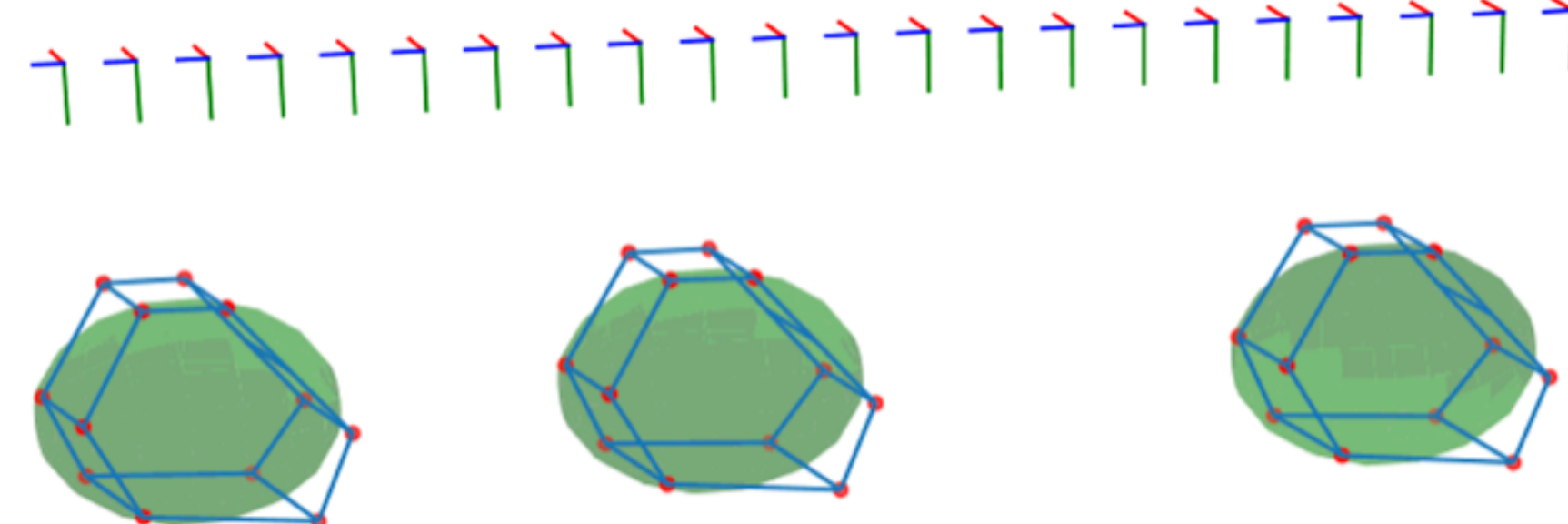
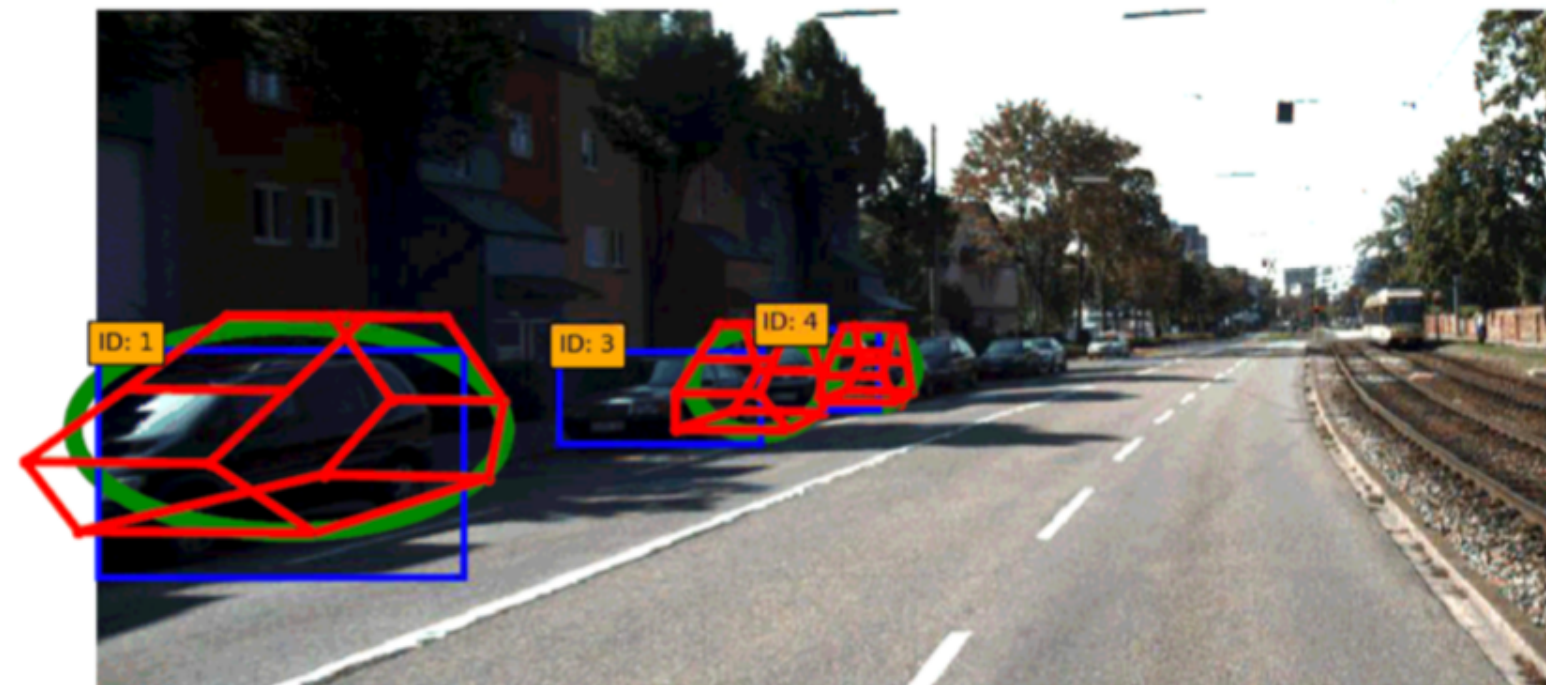
- Object recognition using deep neural networks have impressive results



Motivation

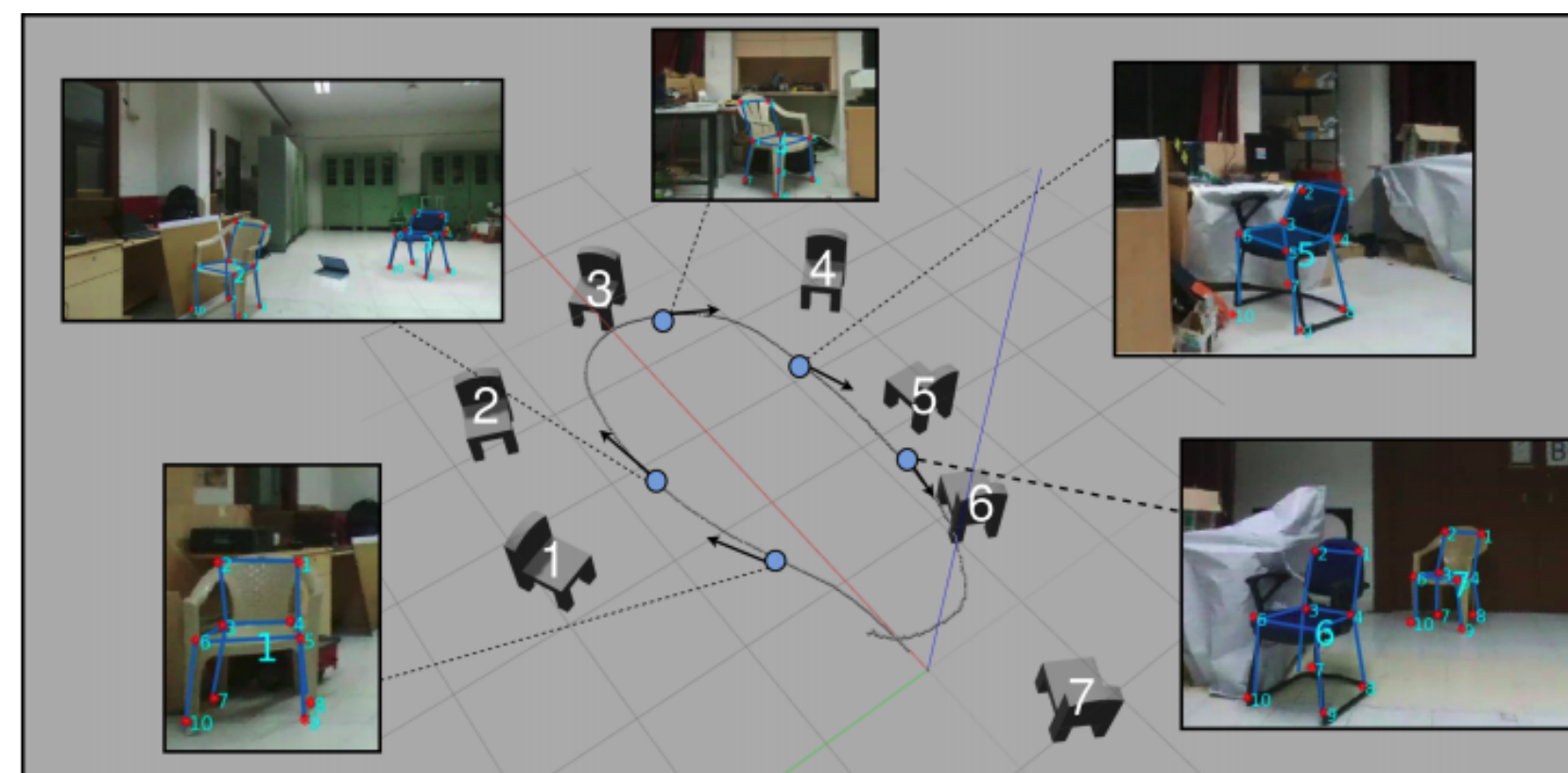
- This work harnesses the strength of both VIO and deep neural networks
- We propose Object residual constrained Visual-Inertial Odometry (OrcVIO)
- OrcVIO outputs geometrically consistent, semantically meaningful maps

OrcVIO

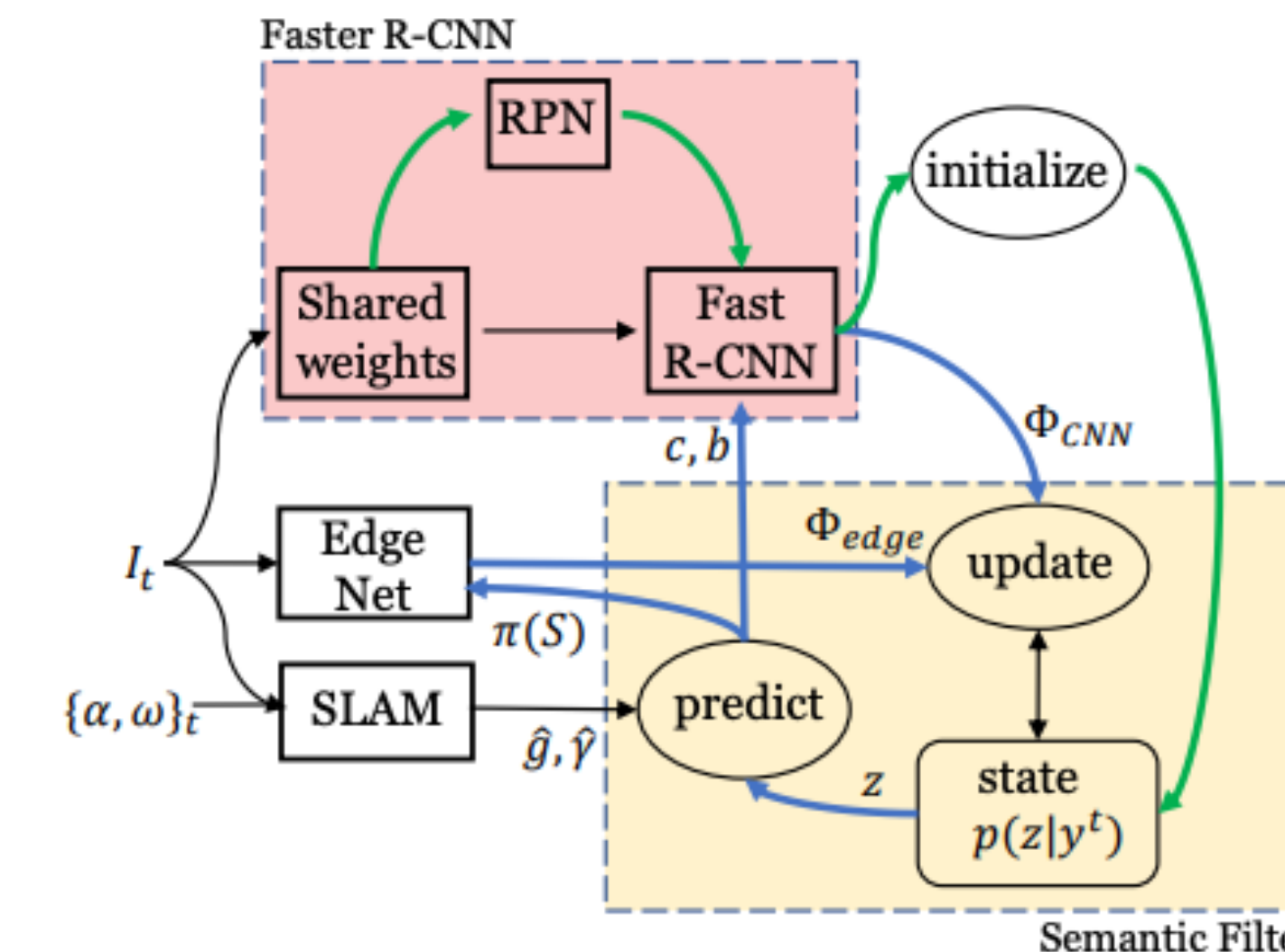


Related Work

- Category-specific approaches optimize the pose and shape of object instances using 3D shape models/semantic keypoints



Parkhiya et al., 2018, ICRA

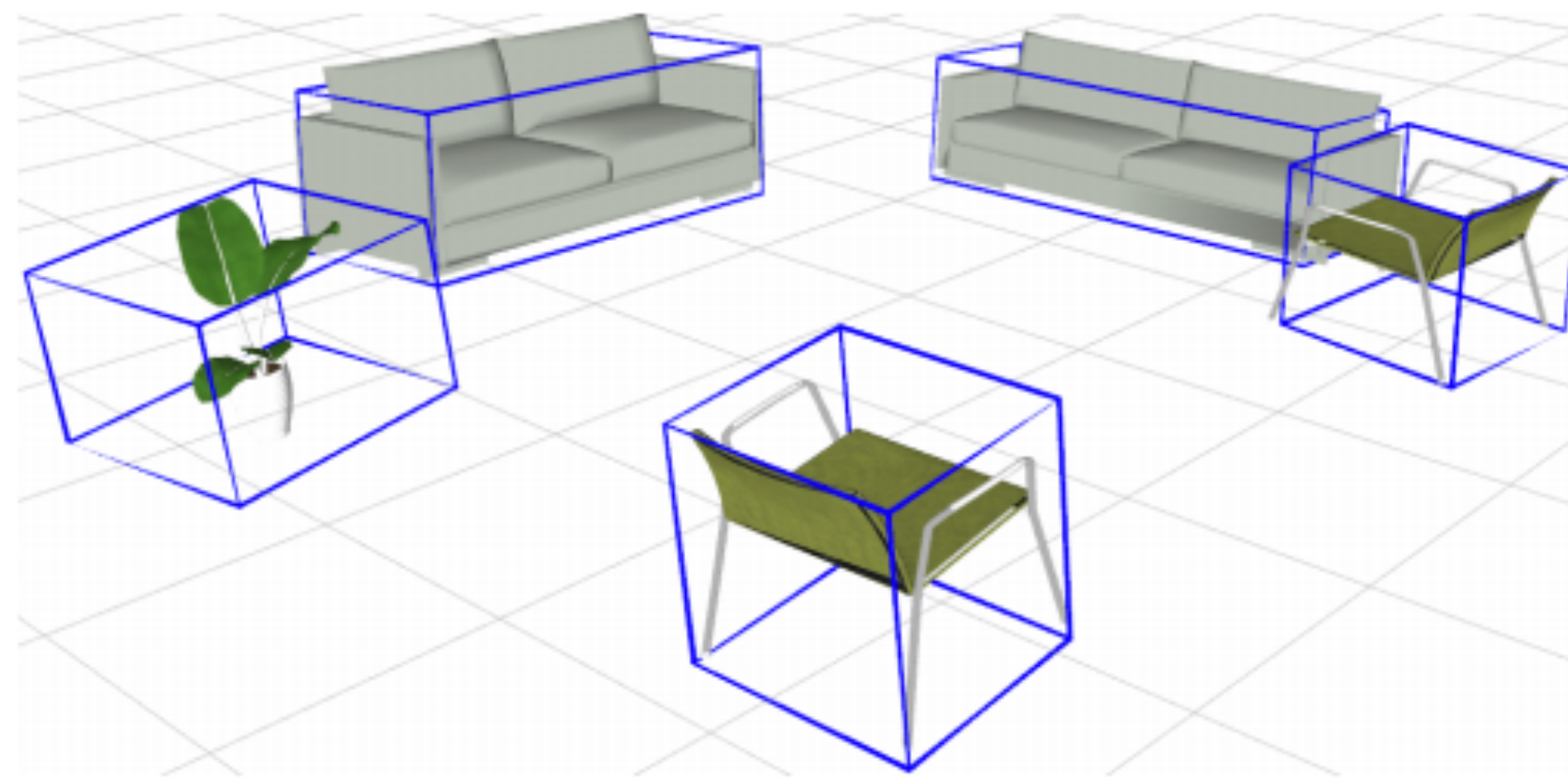


Fei, X., & Soatto, S., 2018, ECCV

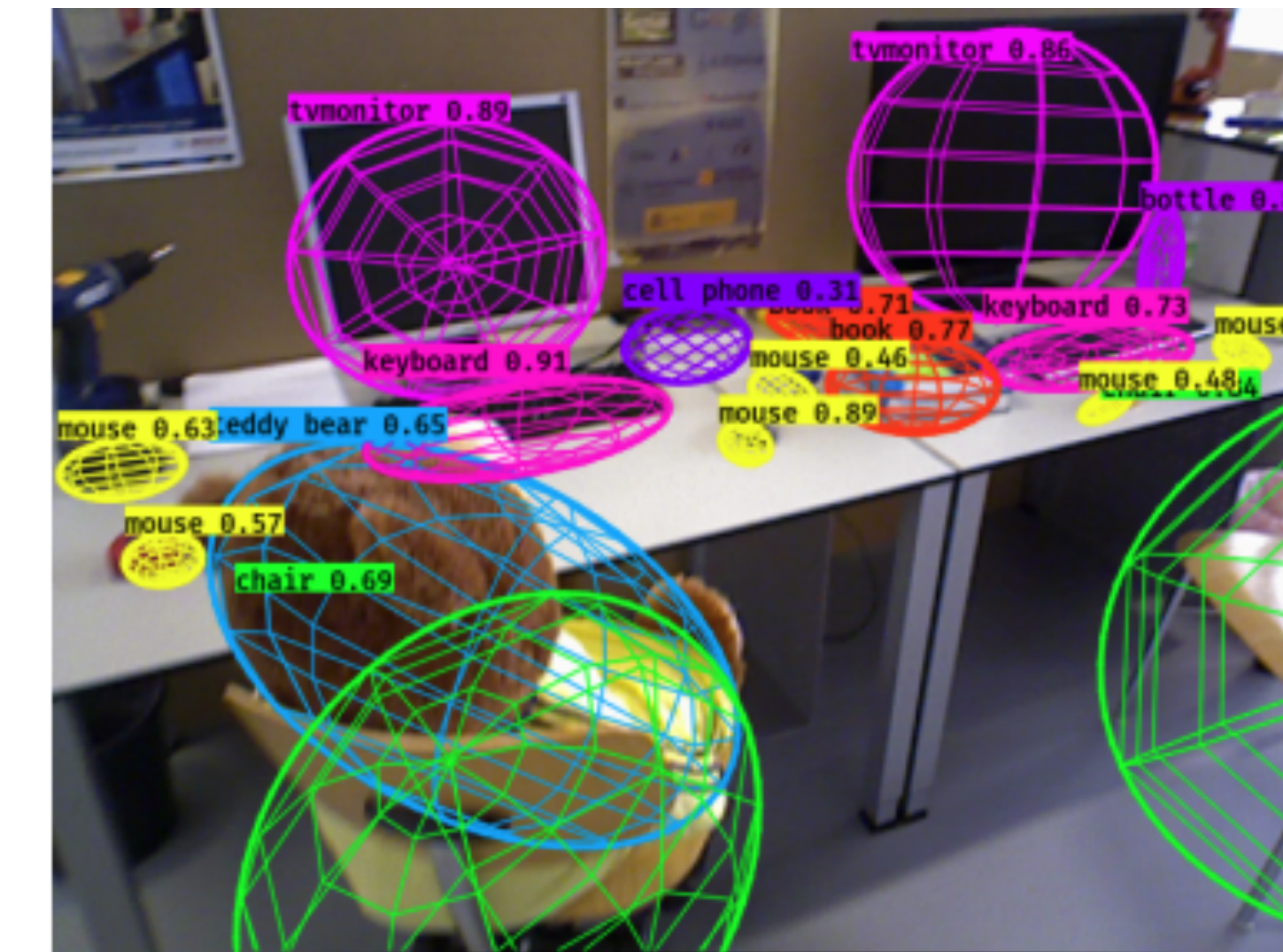
- Parkhiya, P., Khawad, R., Murthy, J.K., Bhowmick, B. and Krishna, K.M., 2018, May. Constructing category-specific models for monocular object-SLAM. In *2018 IEEE International Conference on Robotics and Automation (ICRA)*
- Fei, X. and Soatto, S., 2018. Visual-inertial object detection and mapping. In *Proceedings of the European Conference on Computer Vision (ECCV)* (pp. 301-317).

Related Work

- Category-agnostic approaches use geometric shapes such as ellipsoids or cuboids to represent objects



CubeSLAM, Yang, S. and Scherer, S., 2019, TRO

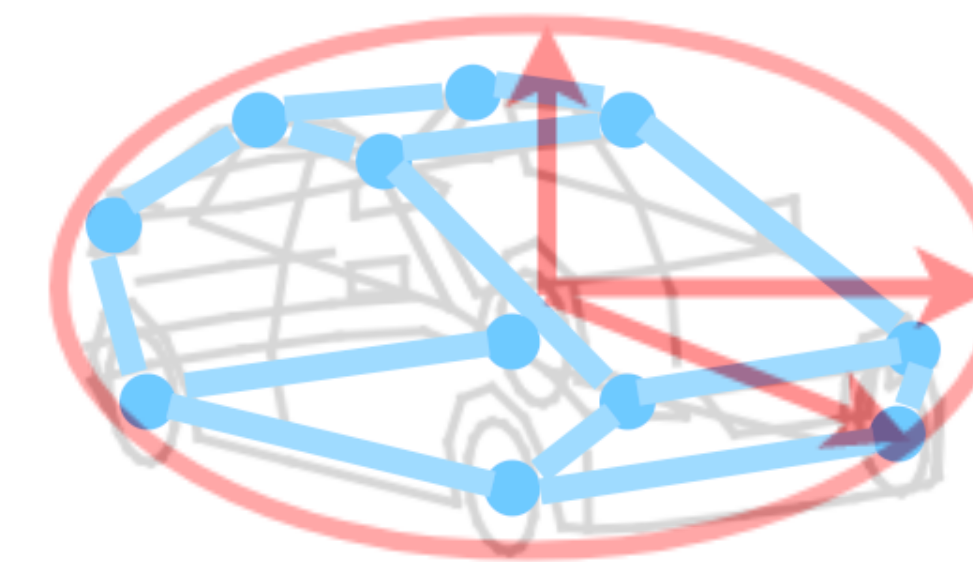


QuadricSLAM, Nicholson et al., 2018, RAL

- Yang, S. and Scherer, S., 2019. Cubeslam: Monocular 3-d object slam. IEEE Transactions on Robotics, 35(4), pp.925-938.
- Nicholson, L., Milford, M. and Sünderhauf, N., 2018. Quadricslam: Dual quadrics from object detections as landmarks in object-oriented slam. IEEE Robotics and Automation Letters, 4(1), pp.1-8.

Object Class

- Coarse level: ellipsoid (red)
- Fine level: keypoints (blue)

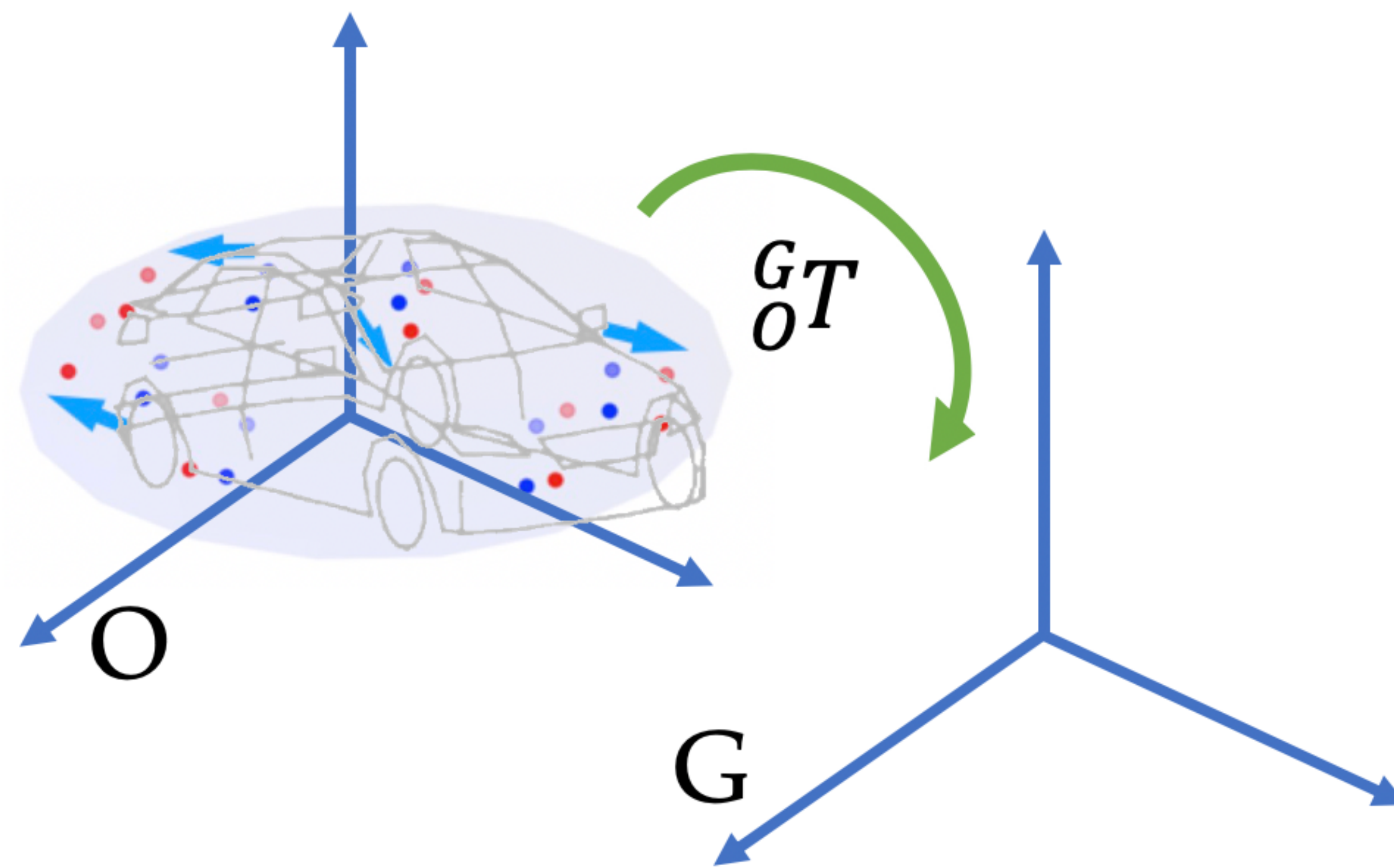


“Treat nature by means of the cylinder, the sphere, the cone, everything brought into proper perspective”

Paul Cezanne

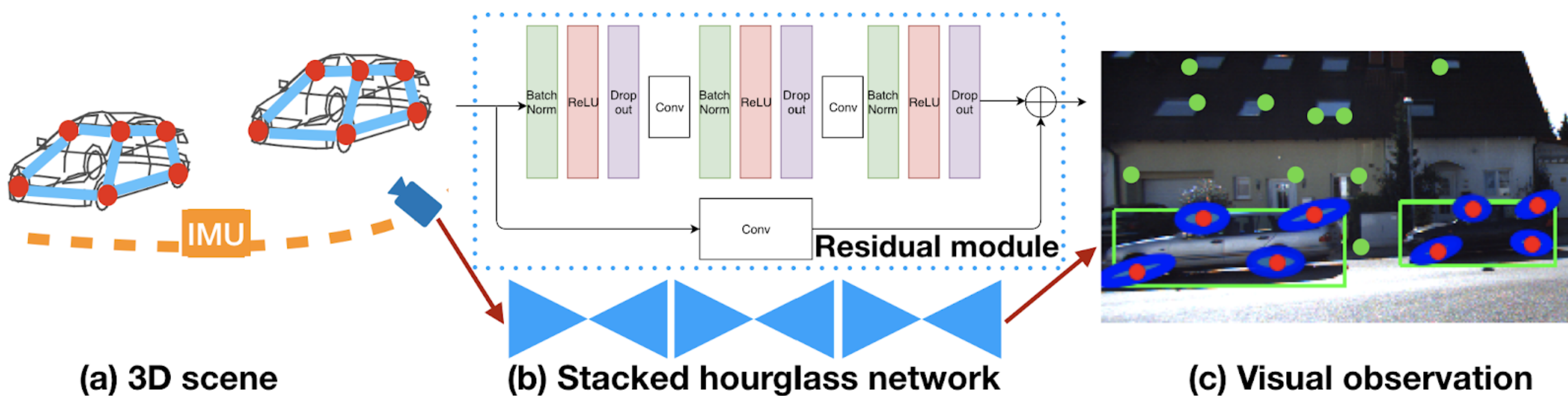
Object Instance

- Deformation (blue arrows)
- Pose (green arrow)



Problem Formulation

- Determine the sensor trajectory, geometric landmarks, and object states using inertial, geometric, semantic, and bounding-box measurements

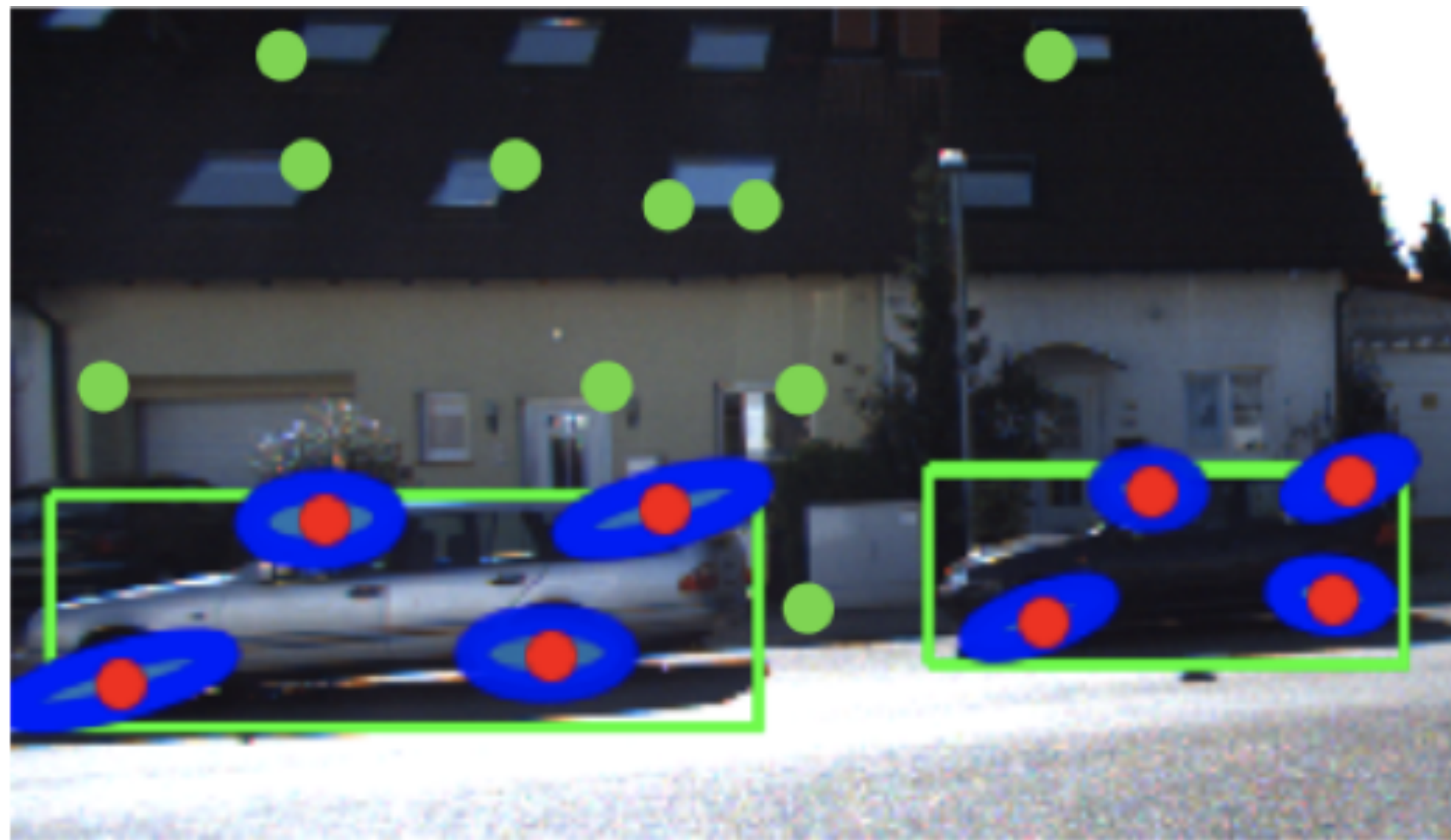

$$\begin{aligned} \text{min } & \text{TrajectoryCost} + \text{GeometricReprojectionCost} + \\ & \text{SemanticReprojectionCost} + \text{BoundingBoxCost} + \\ & \text{ShapeRegularization} \end{aligned}$$

Objective Function

Problem. Determine the sensor trajectory \mathcal{X}^* , geometric landmarks \mathcal{L}^* , and object states \mathcal{O}^* that minimize the weighted sum of squared errors:

$$\begin{aligned} \min_{\mathcal{X}, \mathcal{L}, \mathcal{O}} & {}^i w \sum_t \|{}^i \mathbf{e}_{t,t+1}\|_i^2 \mathbf{v} + {}^g w \sum_{t,m,n} \mathbf{1}_{t,m,n} \|{}^g \mathbf{e}_{t,m,n}\|_g^2 \mathbf{v} \\ & + {}^s w \sum_{t,i,j,k} \mathbf{1}_{t,i,k} \|{}^s \mathbf{e}_{t,i,j,k}\|_s^2 \mathbf{v} + {}^b w \sum_{t,i,j,k} \mathbf{1}_{t,i,k} \|{}^b \mathbf{e}_{t,i,j,k}\|_b^2 \mathbf{v} \\ & + {}^r w \sum_i \|{}^r \mathbf{e}(\mathbf{o}_i)\|^2 \end{aligned}$$

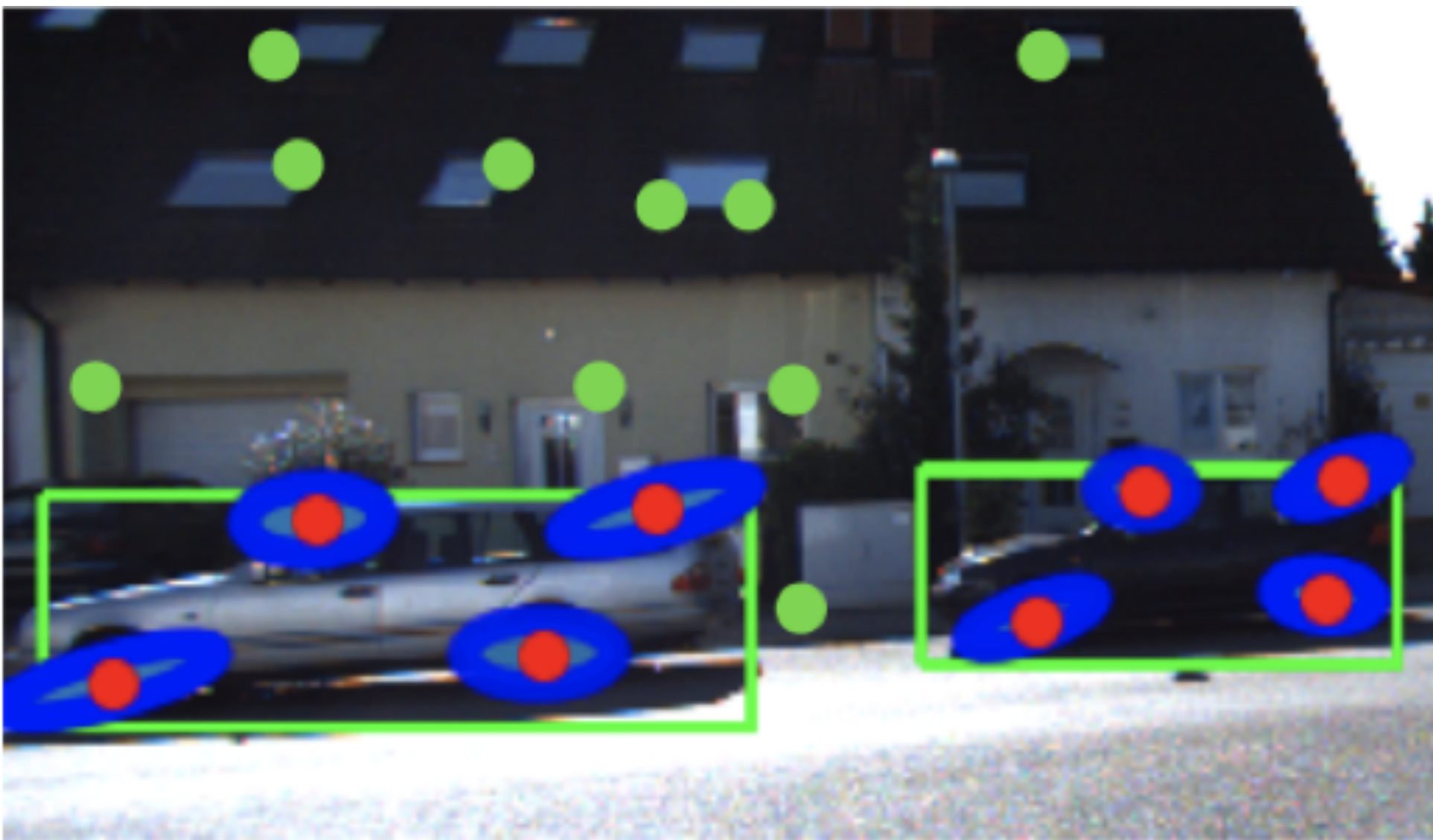
Geometric Keypoints



Define the geometric keypoint error as the difference between the image projection of a geometric landmark ℓ using camera pose ${}_C\mathbf{T}$ and its associated keypoint observation ${}^g\mathbf{z}$:

$${}^g\mathbf{e}(\mathbf{x}, \ell, {}^g\mathbf{z}) \triangleq \mathbf{P}\pi({}_C\mathbf{T}^{-1}\underline{\ell}) - {}^g\mathbf{z},$$

Semantic Keypoints

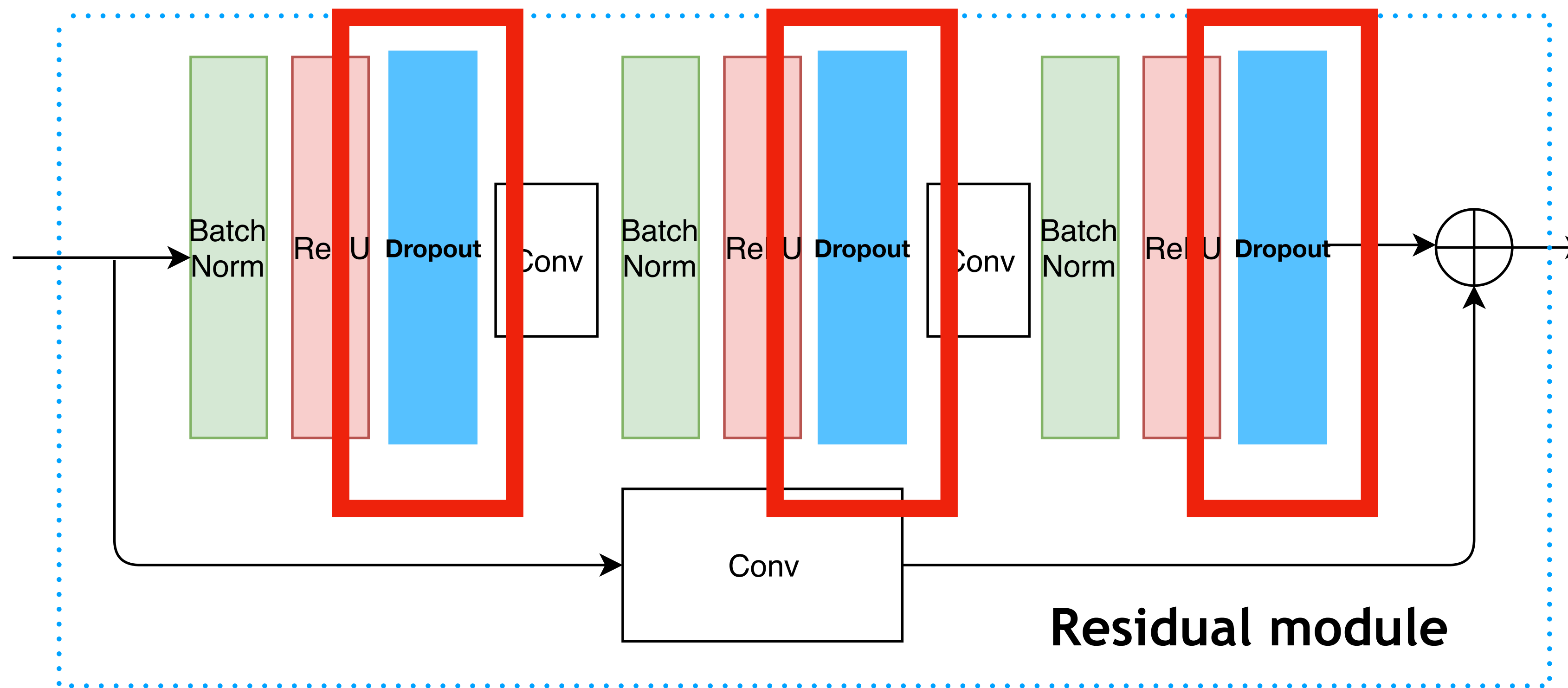


The semantic-keypoint error is defined as the difference between a semantic landmark $\mathbf{s}_j + \delta\mathbf{s}_j$, projected to the image plane using instance pose ${}_O\mathbf{T}$ and camera pose ${}_C\mathbf{T}_t$, and its corresponding semantic keypoint observation ${}^s\mathbf{z}_{t,j,k}$:

$${}^s\mathbf{e}(\mathbf{x}_t, \mathbf{o}, {}^s\mathbf{z}_{t,j,k}) \triangleq \mathbf{P}\pi({}_C\mathbf{T}_t^{-1} {}_O\mathbf{T} (\underline{\mathbf{s}}_j + \delta\underline{\mathbf{s}}_j)) - {}^s\mathbf{z}_{t,j,k}.$$

Semantic Keypoints

- StarMap is used to detect semantic keypoints
- We add drop out layers in original network to obtain covariance



- Zhou, X., Karpur, A., Luo, L. and Huang, Q., 2018. Starmap for category-agnostic keypoint and viewpoint estimation. In *Proceedings of the European Conference on Computer Vision (ECCV)* (pp. 318-334).

Semantic Keypoints

- We use Kalman Filter to track the semantic keypoints on an object level



Object Initialization

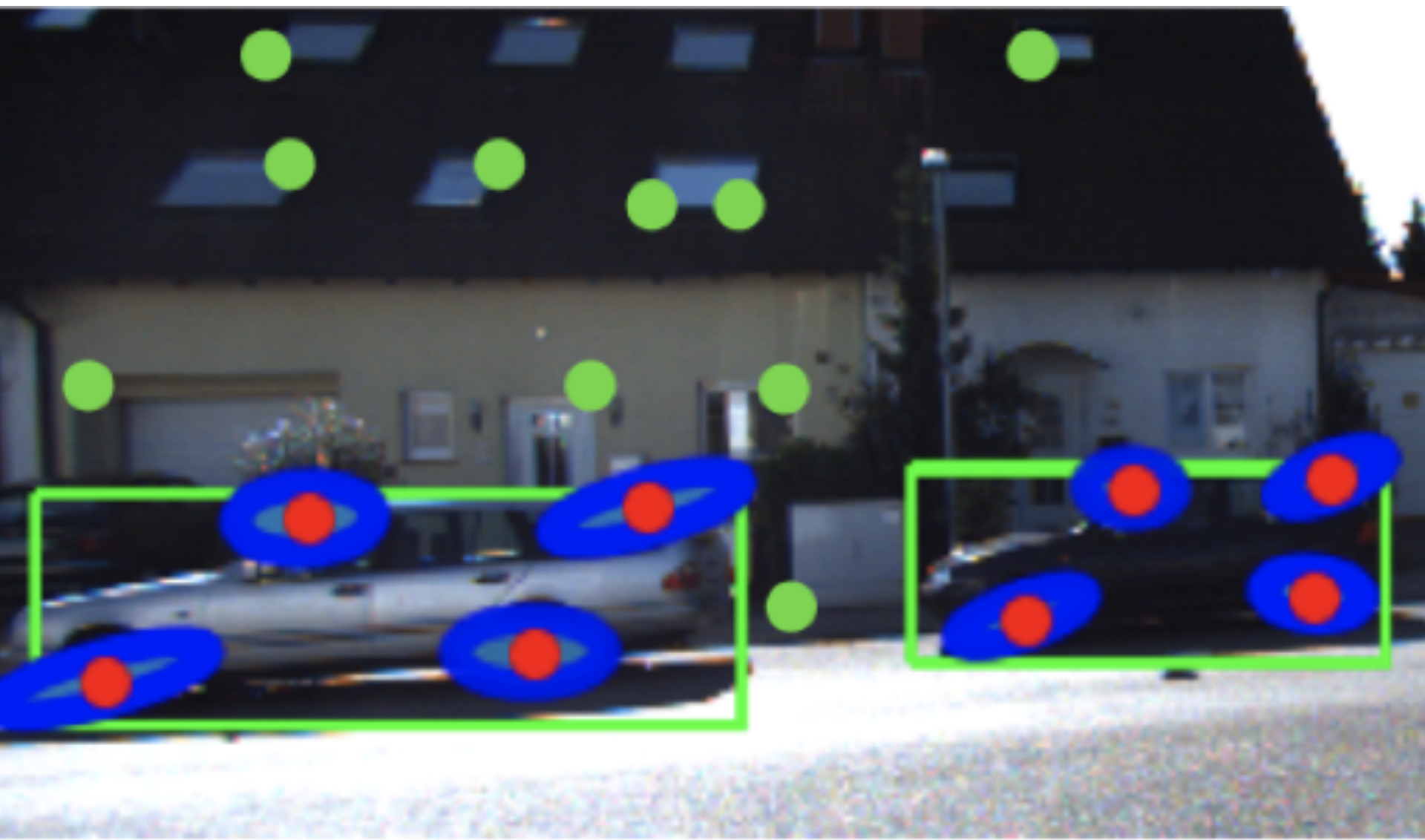
$$\mathbf{0} = \mathbf{P}_C \hat{\mathbf{T}}_t^{-1} {}_O \hat{\mathbf{T}} \underline{\mathbf{s}}_j - \lambda_{t,j,k} {}^s \mathbf{z}_{t,j,k}$$

Rearranging that leads to

$$\begin{aligned} {}_C \hat{\mathbf{R}}_t^\top (\boldsymbol{\xi}_j - {}_C \hat{\mathbf{p}}_t) &= \lambda_{t,j,k} {}^s \mathbf{z}_{t,j,k} \\ {}_C \hat{\mathbf{R}}_t^\top \boldsymbol{\xi}_j - {}^s \mathbf{z}_{t,j,k} \lambda_{t,j,k} &= {}_C \hat{\mathbf{R}}_t^\top {}_C \hat{\mathbf{p}}_t \\ \boldsymbol{\xi}_j - {}_C \hat{\mathbf{R}}_t {}^s \mathbf{z}_{t,j,k} \lambda_{t,j,k} &= {}_C \hat{\mathbf{p}}_t \end{aligned}$$



Bounding-box Measurements



To define a bounding-box error, we observe that if the dual ellipsoid $\mathbf{Q}_{(\mathbf{u}+\delta\mathbf{u})}^*$ of instance \mathbf{i} is estimated accurately, then the lines ${}^b\underline{\mathbf{z}}_{t,j,k}$ of the k -th bounding-box at time t should be tangent to the image plane conic projection of $\mathbf{Q}_{(\mathbf{u}+\delta\mathbf{u})}^*$:

$${}^b\mathbf{e}(\mathbf{x}, \mathbf{o}, {}^b\underline{\mathbf{z}}) \triangleq {}^b\underline{\mathbf{z}}^\top \mathbf{P}_C \mathbf{T}^{-1} O \mathbf{T} \mathbf{Q}_{(\mathbf{u}+\delta\mathbf{u})}^* O \mathbf{T}^\top C \mathbf{T}^{-\top} \mathbf{P}^\top {}^b\underline{\mathbf{z}}.$$

Jacobians

$$\frac{\partial^s \mathbf{e}}{\partial_O \boldsymbol{\xi}} = \mathbf{P} \frac{d\pi}{d\underline{\mathbf{s}}} \left({}_C \hat{\mathbf{T}}_t^{-1} {}_O \hat{\mathbf{T}} \left(\underline{\mathbf{s}}_j + \underline{\delta \hat{\mathbf{s}}}_j \right) \right) {}_C \hat{\mathbf{T}}_t^{-1} \left[{}_O \hat{\mathbf{T}} \left(\underline{\mathbf{s}}_j + \underline{\delta \hat{\mathbf{s}}}_j \right) \right]^\odot$$

$$\frac{\partial^s \mathbf{e}}{\partial \delta \tilde{\mathbf{s}}_j} = \mathbf{P} \frac{d\pi}{d\underline{\mathbf{s}}} \left({}_C \hat{\mathbf{T}}_t^{-1} {}_O \hat{\mathbf{T}} \left(\underline{\mathbf{s}}_j + \underline{\delta \hat{\mathbf{s}}}_j \right) \right) {}_C \hat{\mathbf{T}}_t^{-1} {}_O \hat{\mathbf{T}} \begin{bmatrix} \mathbf{I}_3 \\ \mathbf{0}^\top \end{bmatrix} \in \mathbb{R}^{2 \times 3}.$$

$$\frac{\partial^b \mathbf{e}}{\partial_O \boldsymbol{\xi}} = 2^b \underline{\mathbf{z}}^\top \mathbf{P} {}_C \hat{\mathbf{T}}_t^{-1} {}_O \hat{\mathbf{T}} \hat{\mathbf{Q}}_{(\mathbf{u} + \delta \hat{\mathbf{u}})}^* {}_O \hat{\mathbf{T}}^\top \left[{}_C \hat{\mathbf{T}}_t^{-\top} \mathbf{P}^\top {}^b \underline{\mathbf{z}} \right]^\odot$$

$$\frac{\partial^b \mathbf{e}}{\partial \delta \tilde{\mathbf{u}}} = (2(\mathbf{u} + \delta \hat{\mathbf{u}}) \odot \mathbf{y} \odot \mathbf{y})^\top \in \mathbb{R}^{1 \times 3}$$

$$\mathbf{y} \triangleq \begin{bmatrix} \mathbf{I}_3 & \mathbf{0} \end{bmatrix} {}_O \hat{\mathbf{T}}^\top {}_C \hat{\mathbf{T}}_t^{-\top} \mathbf{P}^\top {}^b \underline{\mathbf{z}}.$$

Visual-Inertial Odometry

- We propose a framework similar to MSCKF for fusing the visual and inertial observations to estimate the robot states
- Instead of using quaternion, we use rotation matrix to parameterize the robot state

$${}^I \mathbf{X}_t \triangleq ({}^I \mathbf{R}_t, {}^I \mathbf{P}_t, {}^I \mathbf{V}_t, \mathbf{b}_g, \mathbf{b}_a)$$

- Moreover, we have derived a closed-form integration to propagate the robot state

$$\begin{aligned} {}^I \hat{\mathbf{p}}_{t+1}^p &= {}^I \hat{\mathbf{p}}_t + {}^I \hat{\mathbf{v}}_t \tau + \mathbf{g} \frac{\tau^2}{2} + {}^I \hat{\mathbf{R}}_t \mathbf{H}_L \left(\tau ({}^i \boldsymbol{\omega}_t - \hat{\mathbf{b}}_{g,t}) \right) ({}^i \mathbf{a}_t - \hat{\mathbf{b}}_{a,t}) \tau^2 \\ {}^I \hat{\mathbf{v}}_{t+1}^p &= {}^I \hat{\mathbf{v}}_t + \mathbf{g} \tau + {}^I \hat{\mathbf{R}}_t \mathbf{J}_L \left(\tau ({}^i \boldsymbol{\omega}_t - \hat{\mathbf{b}}_{g,t}) \right) ({}^i \mathbf{a}_t - \hat{\mathbf{b}}_{a,t}) \tau \end{aligned}$$

$$\mathbf{J}_L(\boldsymbol{\omega}) = \mathbf{I}_3 + \frac{1 - \cos \|\boldsymbol{\omega}\|}{\|\boldsymbol{\omega}\|^2} \boldsymbol{\omega}_{\times} + \frac{\|\boldsymbol{\omega}\| - \sin \|\boldsymbol{\omega}\|}{\|\boldsymbol{\omega}\|^3} \boldsymbol{\omega}_{\times}^2$$

$$\mathbf{H}_L(\boldsymbol{\omega}) = \frac{1}{2} \mathbf{I}_3 + \frac{\|\boldsymbol{\omega}\| - \sin \|\boldsymbol{\omega}\|}{\|\boldsymbol{\omega}\|^3} \boldsymbol{\omega}_{\times} + \frac{2(\cos \|\boldsymbol{\omega}\| - 1) + \|\boldsymbol{\omega}\|^2}{2\|\boldsymbol{\omega}\|^4} \boldsymbol{\omega}_{\times}^2.$$

Qualitative Results

- Backprojection of estimated keypoints and ellipsoid



Quantitative Results

TABLE II
PRECISION-RECALL EVALUATION ON KITTI OBJECT SEQUENCES

Translation error →		≤ 0.5 m		≤ 1.0 m		≤ 1.5 m	
Rotation error	Method	Precision	Recall	Precision	Recall	Precision	Recall
$\leq 30^\circ$	SubCNN [36]	0.10	0.07	0.26	0.17	0.38	0.26
	VIS-FNL [14]	0.14	0.10	0.34	0.24	0.49	0.35
	OrcVIO	0.10	0.12	0.18	0.21	0.22	0.25
$\leq 45^\circ$	SubCNN [36]	0.10	0.07	0.26	0.17	0.38	0.26
	VIS-FNL [14]	0.15	0.11	0.35	0.25	0.50	0.36
	OrcVIO	0.15	0.17	0.25	0.28	0.31	0.35
–	SubCNN [36]	0.10	0.07	0.27	0.18	0.41	0.28
	VIS-FNL [14]	0.16	0.11	0.40	0.29	0.58	0.42
	OrcVIO	0.29	0.33	0.50	0.56	0.62	0.69

Thank you!



http://me-llamo-sean.cf/orcvio_githubpage/



Mo Shan
moshan@ucsd.edu



UC San Diego
JACOBS SCHOOL OF ENGINEERING
Electrical and Computer Engineering